FIA 2018
XI Congreso Iberoamericano de Acústica; X Congreso Ibérico de Acústica; 49º Congreso Español de Acústica -TECNIACUSTICA'18-
24 al 26 de octubre

SBM ANALYSIS OF THE INFLUENCE OF BONE-SHAPE IN THE TARGET STRENGTH OF A FISH

PACS: 43.30.+m

Godinho, Luís[1]; Perez-Arjona, Isabel[2]; Espinosa, Victor[2]

[1]ISISE, Departamento de Engenharia Civil, Universidade de Coimbra
Rua Luís Reis Santos - Pólo II da Universidade, 3030-788 Coimbra, Portugal
{capa@uc.pt, lgodinho@dec.uc.pt}

[2]Institut d'Investigació per a la Gestió Integrada de Zones Costaneres
Universitat Politècnica de València
{ iparjona@upv.es, vespinos@upv.es }

Keywords: target strength, SBM, fishbone features

ABSTRACT

Existing works have addressed the target strength (TS) of a fish using different experimental and numerical strategies, and assessing different configurations. Here, we propose the application of a numerical model based on the Singular Boundary Method (SBM) to analyse the effect of considering a realistic irregular geometry for the fish bone in the TS evaluation. In particular, it is sought to understand the possible effect of the irregularities in the cancellation of coherent field effects that may occur when a regular cylindrical bone is considered.

RESUMO

Muitos trabalhos existentes abordam o "target strength" (TS) de um peixe usando diferentes estratégias numéricas e experimentais, e avaliando diferentes configurações. Aqui, propomos a aplicação de um modelo numérico baseado no "singular boundary method" (SBM) para analisar o efeito de considerar uma geometria irregular realista para a espinha de um peixe na avaliação TS. Em particular, procura-se compreender o possível efeito das irregularidades no cancelamento de efeitos de campo coerentes que podem ocorrer quando se considera uma espinha cilíndrica regular.

INTRODUCTION

The target strength (TS) is one of the most used parameters for active detection in underwater acoustics [1]. This parameter indicates the capacity of a given target to reflect back the incident acoustic energy, and thus it can be seen as a quantitative value of the reflectivity of the target. TS value depends both on the object properties and on the acoustic frequency, being an important value to quantify underwater targets. The TS parameter is widely applied in the area

of fisheries, measuring the acoustic reflectivity of a fish. Besides being dependent on the frequency, its value is also quite dependent on a number of physical variables such as species, size, shape, orientation or depth and it is one of the most important inputs to study acoustically fish populations [2]. Several researchers proposed the use of TS to monitor the fish growing in aquaculture cages, and also to verify if intruder species enter the aquaculture cage [3]. Although it is known that the main contribution to the TS value in swim-bladdered fish comes from the swimbladder (which is gas-filled and thus presents a large acoustic contrast to the surrounding media), other parts of the fish can also influence the measured value of the TS. When those fishes are insonified from above (dorsal insonification), the contribution of the fishbone can becom more important, and the TS may be quite dependent from it. In fact, in fish which do not possess a swimbladder (as is the case, for example, of the Atlantic mackerel (*Scomber scombrus*, Linnaeus 1758)) the main contributions to the acoustic echo come from other structures, such as the flesh or the fish-bone. In a previous paper by the authors, the influence of the various structures in the acoustic scattering by swim-bladdered fish was studied using the Method of Fundamental Solutions (MFS) [4]. However, in that case, simplified geometries of each part of the fish were used, and thus it was not possible to assess the influence of details in the final scattered field.

Numerical models have been widely used to estimate the TS of fish, trying to interpret the influence of the various features and structures in the acoustic field. In many cases, the numerical simulations can be useful when interpreting TS experimental results in ex-situ and in-situ TS measurements. For the case of the effect of the swimbladder, a comparison of the results obtained using well stablished numerical models was developed in [5], approximating the swimbladder by prolate spheroids with pressure release conditions, and comparing the result from the analytically exact prolate-spheroid-modal-series model (PSMS), from the Kirchhoff-approximation (KA), from Kirchhoff-ray-mode (KRM), and from the Helmholtz equation solution using finite elements (FE). The above mentioned study [4] by the authors of the present paper presents a detailled study on the influence of the various structures using a newly developed MFS model, and comparing it with other well established numerical tools, such as the Boundary Element Method (BEM). Although quite versatile, the MFS poses some difficulties when dealing with intricate geometries, as it relies on a number of virtual sources, placed outside the propagation domain, to simulate the acoustic wavefield; when complex geometries need to be assessed, defining the position of such sources can be challenging.

In this paper the authors implement, verify and apply a more recent variant of the MFS, named the Singular Boundary Method (SBM), to study the effect modelling the fish-bone in a more detailled manner in the TS results. The SBM derives directly from the MFS, but considers the virtual sources to be positioned directly at the boundary, and thus avoiding the difficulty of defining a good location for those sources. Several references can be found regarding the application of the SBM in acoustics, such as the work by Chen and Wang [6], Fu et al [7] or Qu et al [8], which demonstrate its general applicability to solve the Helmholtz equation. The paper is organized as follows: first, a brief overview of the formulation of the SBM is given; then, a verification is presented by comparing its results with those computed analytically for the case of a fluid-filled sphere; finally, some numerical simulations regarding the acoustic scattering by differently shaped fish-bones are discussed.

MATHEMATICAL FORMULATION OF THE SBM

The propagation of sound within a homogeneous acoustic space can be mathematically represented in the frequency domain by the Helmholtz differential equation,

$$\nabla^2 p + k^2 p = 0 \qquad (1)$$

where $\nabla^2 = \frac{\partial^2}{\partial x^2} + \frac{\partial^2}{\partial y^2} + \frac{\partial^2}{\partial z^2}$ in the case of a 3D problem; *p* is the acoustic pressure, $k = \omega/c$ the wave number, $\omega = 2\pi f$ the angular frequency, f the frequency and *c* the sound propagation velocity within the acoustic medium.

For the 3D case, assuming a point source placed within the propagation domain, at point $\boldsymbol{x_0}$ with coordinates (x_0, y_0, z_0), it is possible to establish fundamental solutions *G*, for the sound pressure, and *H*, for the particle velocity, at a point $\boldsymbol{x}$ with coordinates (x, y, z), which can be written respectively as:

$$G^{3D}(\boldsymbol{x}, \boldsymbol{x}_0, k) = \frac{\mathrm{e}^{-\mathrm{i}kr}}{r}, \quad (2)$$

$$H^{3D}(\boldsymbol{x}, \boldsymbol{x}_0, k, \vec{n}) = \frac{1}{-\mathrm{i}\rho\omega} \frac{(-\mathrm{i}kr - 1)\mathrm{e}^{-\mathrm{i}kr}}{r^2} \frac{\partial r}{\partial \vec{n}}. \quad (3)$$

In these equations, *r* corresponds to the distance between the source point and the domain point, given; $\vec{n}$ represents the direction along which the particle velocity is calculated and ρ the medium density.

In the present paper, the problem to be solved consists of an infinite homogeneous fluid medium within which a fluid-filled scatterer is located. To model the presence of the scatterer, the SBM will here be used. To formulate the SBM for the analysis of acoustic scattering, it is first necessary to understand that the basic principle of the SBM is that the sound field in a homogeneous region can be simulated by the linear superposition of the effects of a number NS of virtual sources, each one with its own amplitude, placed directly over the interface between the host medium and the scatterer. Given this initial definition, the acoustic field in the host fluid can be seen as the linear combination of the effects of NS acoustic sources, distributed throughout the surface of the scatterer.

$$p(\boldsymbol{x}, k)_{\Omega_1} = \sum_{j=1}^{NS} P_j G^{3D}(\boldsymbol{x}, \boldsymbol{x}_1, k_1) + p_{inc}(\boldsymbol{x}, \boldsymbol{x}_{source}, k_1) \text{ for } \boldsymbol{x} \text{ in } \Omega_1 \quad (4)$$

Inside the fluid filled-scatterer, the acoustic field can be described in a similar manner as:

$$p(\boldsymbol{x}, k)_{\Omega_2} = \sum_{j=1}^{NS} Q_j G^{3D}(\boldsymbol{x}, \boldsymbol{x}_j, k_2) + p_{inc}(\boldsymbol{x}, \boldsymbol{x}_{source}, k_2) \text{ for } \boldsymbol{x} \text{ in } \Omega_2 \quad (5)$$

In equations (4) and (5), P_j and Q_j correspond to the unknown amplitudes of the virtual sources, and $p_{inc}(\boldsymbol{x}, \boldsymbol{x}_{source}, k)$ represents the incident field generated by a source located at $\boldsymbol{x}_{source}$, and k_1 and k_2 represent the wavenumber in the host medium (water), or inside the scatterer, respectively. To determine the relevant amplitudes, a system of equations must be established by imposing the necessary interface and boundary conditions, which correspond to continuity of pressure and normal velocity throughout the interface. To impose those conditions, a number of collocation points are considered throughout the surfaces of the scatterer, coincident with the virtual sources, as depicted in Figure 1. An equation system then arises, which can be schematically represented as in equation (6).

$$\mathbf{A}\mathbf{x} = \mathbf{B} \Leftrightarrow \begin{bmatrix} \mathbf{G}_{\Gamma,\Omega_1} & -\mathbf{G}_{\Gamma,\Omega_2} \\ \mathbf{H}_{\Gamma,\Omega_1} & -\mathbf{H}_{\Gamma,\Omega_2} \end{bmatrix} \begin{bmatrix} \mathbf{P} \\ \mathbf{Q} \end{bmatrix} = \begin{bmatrix} -\mathbf{p}_{inc,\Gamma} \\ -\mathbf{v}_{inc,\Gamma} \end{bmatrix} \quad (6)$$

In this equation, $\mathbf{G}_{\Gamma,\Omega_1}$ and $\mathbf{H}_{\Gamma,\Omega_1}$ represents NSxNS submatrices containing the effects of the virtual sources at the collocation points, coming from the each of the subdomains Ω_1 and Ω_2. For example, each entry of $\mathbf{G}_{\Gamma,\Omega_1}$ can be seen as $\mathbf{G}_{\Gamma,\Omega_1[i,j]} = G^{3D}(\boldsymbol{x}_i, \boldsymbol{x}_j, k_1)$, while for the submatrix $\mathbf{H}_{\Gamma,\Omega_1}$, $\mathbf{H}_{\Gamma,\Omega_1[i,j]} = H^{3D}(\boldsymbol{x}_i, \boldsymbol{x}_j, k_1, \vec{n}_i)$.

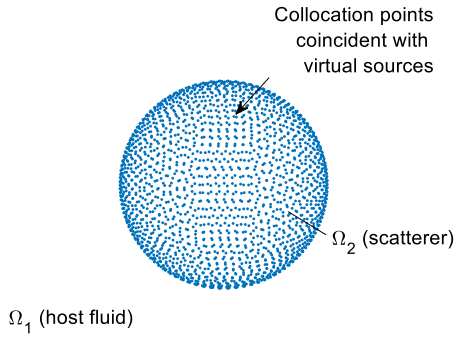

Figure 1 – Schematic representation of the problem.

One particular problem of the SBM occurs for the diagonal terms of each submatrix, for which $\boldsymbol{x}_i \equiv \boldsymbol{x}_j$. Due to the coincidence between source and collocation point, the fundamental solutions of equations (2) and (3) become singular, and cannot be computed. However, to circunvent this problem we here follow the proposal by Qu et al. [8], and compute such terms as average values of the integral of such functions over the influence region (with area A_i) of each virtual source.

$$\mathbf{G}_{\Gamma,\Omega_1[i,i]} = \frac{1}{A_i}\int_{\Gamma_i} G^{3D}(\boldsymbol{x}, \boldsymbol{x}_i, k_1)d\Gamma \quad (7)$$

$$\mathbf{H}_{\Gamma,\Omega_1[i,i]} = \frac{1}{A_i}\left(\frac{C}{2} + \int_{\Gamma_i} H^{3D}(\boldsymbol{x}, \boldsymbol{x}_i, k_1, \vec{n}_i)d\Gamma\right) \quad (8)$$

For equation (8), an additional term $\frac{C}{2}$ arises, for which $C=1$ for the exterior problem, and $C=-1$ for the interior problem, assuming the normal $\vec{n}_i$ to point to the interior of the scatterer. If such region is assumed to be circular and planar, then these integral can be calculated analytically (in fact, for equation (8) the integral becomes null).

VERIFICATION OF THE NUMERICAL METHOD

To verify the correctness of the proposed SBM formulation, the case of a fluid-filled sphere illuminated by an incident plane wave is considered, for which an analytical solution is known [9]. Two different cases are considered, namelly one with a strong property contrast between the inner fluid and the host domain, and another with smaller constrast of properties. Table 1 summarizes those properties.

To verify the correctness of the proposed SBM formulation, the case of a fluid-filled sphere illuminated by an incident plane wave is considered, for which an analytical solution is known [9]. A sphere with radius 0.01 m is considered, illuminated by a plane wave with a frequency of 120 kHz travelling in the negative direction of the x axis; 600 collocation points are used to

model the sphere, and the response is computed over a grid of receivers placed in the x-y plane, at z=0.0 m. Two different cases are considered, namelly one with a strong property contrast between the inner fluid and the host domain, and another with smaller constrast of properties. Table 1 summarizes those properties.

Table 1 – properties used in the verification example

	c (m/s)	ρ (kg/m^3)
Host fluid	1490.0	1030.0
Scatterer - Case 1	4500.0	3000.0
Scatterer - Case 2	2200.0	1090.0

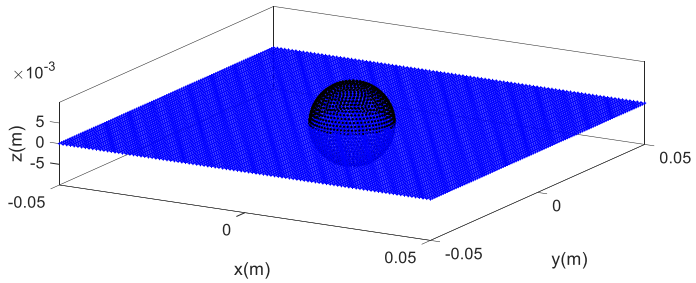

Figure 2 – Geometry of the verification case.

Figure 3 illustrates the results computed for the two test cases, in terms of the absolute pressure value over the grid of receivers, and of the absolute error with respect to the analytical solution ($\left|p_{analytical} - p_{SBM}\right|$). As can be seen in the presented plots, a very good agreement between the numerical and analytical results was found, indicating that the SBM can produce accurate results for both test cases.

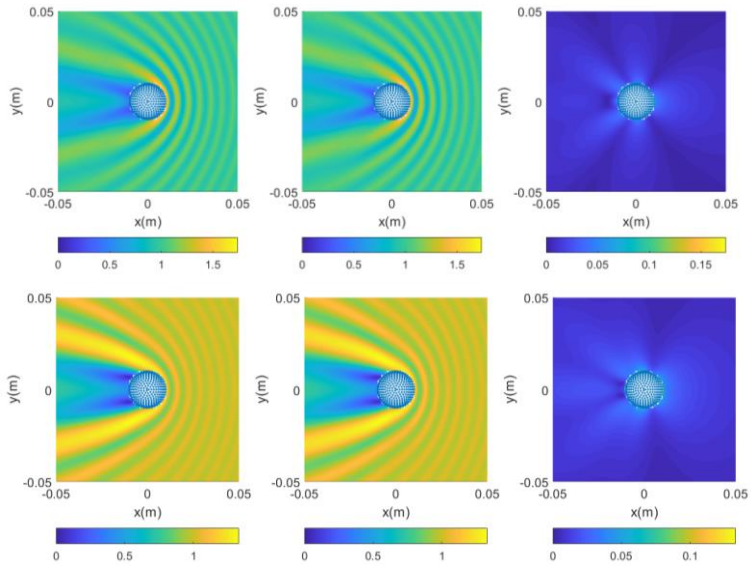

Figure 3 – Numerical SBM (left), analytical (middle) and absolute error (right) values of the absolute pressure over the grid of receivers, when the sphere is modelled with 600 collocation points: a) Case 1; b) Case 2.

NUMERICAL SIMULATIONS

The above described numerical method has been applied to study the scattered field by fish-bone models of two different species: gilt-head sea bream (*Sparus aurata*) and Atlantic salmon (*Salmo salar*). For both species, two models are evaluated for incident sound waves with 70 kHz and 120 kHz, one with a smooth regular shape and the other with an irregularly shaped fish-bone. Fish with around 30 cm total length are considered. Figure 4 illustrates the models used in this analysis.

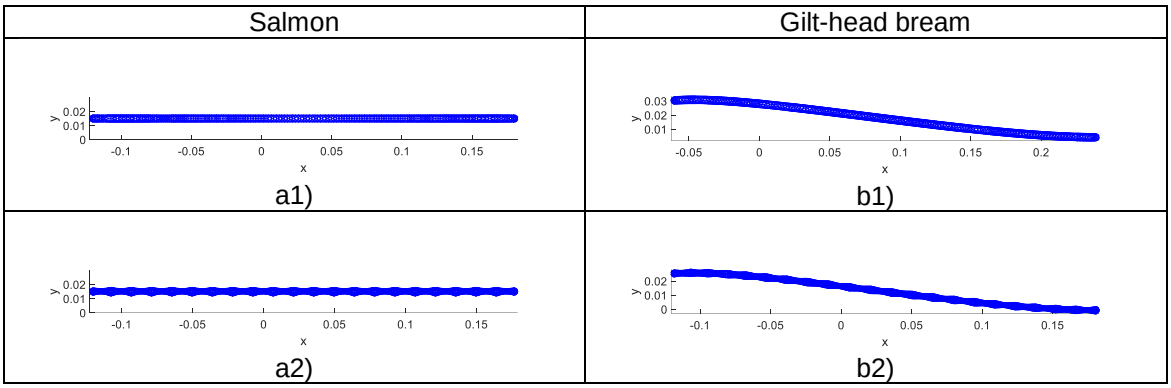

Figure 4 – Geometry of the fishbone used in the numerical simulations. In (a) and (b) the conceptual models of salmon and gilt-head sea bream fishbone are shown; (a1) and (b1) correspond to regular (cylindrical) fishbone and (a2) and (b2) to more detailled models.

The aim of the presented simulations is to observe the effect of spine irregularities. Since both fish species have a swimbladder, and since for ventral insonification the swimbladder clearly dominates the scattering [4], only dorsal insonification is considered here, modeling the situation for which the spine would be the most important. One should note that in order to understand correctly the effect of the spine, and to avoid the interaction with other structures, only the fishbone itself is modeled. For that structure, a propagation velocity of 2200 m/s is assumed, together with a density of 1090 kg/m^3.

Figure 5 illustrates the far-field directivity of the TS computed for the four geometries, and for frequencies of 70 kHz and 120 kHz. Observing those figures, it is quite evident that the main central lobe structure is very similar for irregular and regular fishbone shapes, and that only at wider angles some differences are registered. It is interesting to note that the curved nature of the fishbone of the gilt-head bream leads to a non-normal dominant reflection, which was very much expected. It should be noted that the TS directivity plots computed for 120 kHz for both fish species reveal some strong lateral lobes, with very significant amplitudes, which do not appear for regular fishbone shapes. Indeed, the position of these lateral lobes is related to the periodicity of the irregular shape, as depicted in Figures 4a2 and 4b2. For the case of the gilt-head bream, it can also be seen that the curved nature of the spine leads to a stronger lobe on one of the sides (with the peak ocurring between 0º and 30º).

To have a global view of the near field effect that occurs when the insonification is performed at operating distances like those involved in aquaculture cages, Figure 6 shows the maximum TS registered for distances to the fish between 1 m and 20 m, and for the two frequencies mentioned above. It is interesting to note that the curves follow very similar trends, with and without the irregularities, and that in all cases the value of TS is lower when the irregular fishbone is considered. Maximum differences of around 1.5 dB are registered for the gilt-head sea bream when the lower insonification frequency is considered. At the higher frequency, part of these differences may be a consequence of the dispersion of energy to the lateral directions observed in the polar plots of Figure 5.

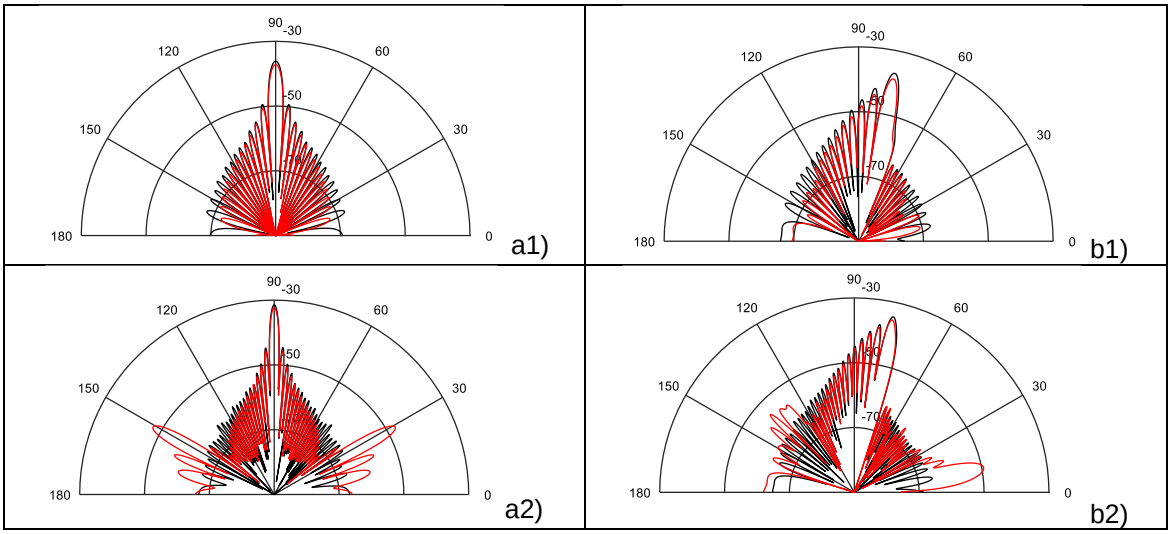

Figure 5 – TS directivity plots of the irregular fishbone for an incident frequency of 70 kHz (a1 and b1) and 120 kHz (a2 and b2); as above, (a) corresponds to the salmon and (b) to the gilt-head bream. Red curves correspond to irregular bone shapes and black curves to regular cylindrical fishbone.

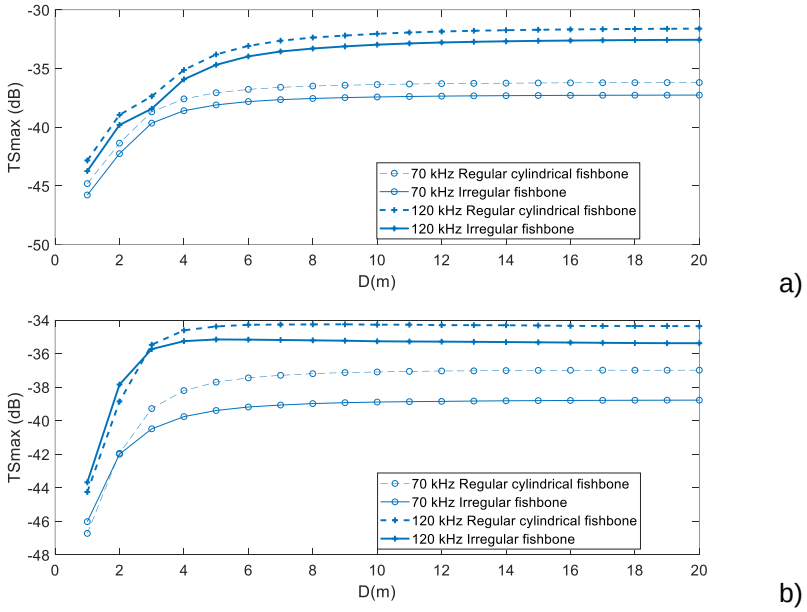

Figure 6 – Maximum TS values as a function of the source-scatterer distance for salmon (a) and gilt-head bream (b).

CONCLUSIONS

This work focused on the numerical modelling of fishbone using a new numerical method – the Singular Boundary method. The method was here presented and verified, reveeling good results when compared to a reference analytical solution. Application of the SBM to model fishbone of two different fish species was demonstrated, and some illustrative results were presented. In that context, it was shown that considering a more detailled geometry for the fishbone leads to some visible changes in the scattered field, and when high insonification

frequencies are considered, to the formation of lateral lobes in the directivy plots. Analysis of the maximum TS for different insonification distances revealed that a small reduction of the TS may occur due to energy dispersion when detailled models of the fishbone are considered. It should be mentioned that the present work does not include the effect of the swimbladder, which can be significant in the studied species, and thus should be seen as an initial approach to the problem, which requires more in-depth studies.

ACKNOWLEDGEMENTS

This work was financed by FEDER funds through the Competitivity Factors Operational Programme - COMPETE and by national funds through FCT – Foundation for Science and Technology within the scope of project POCI-01-0145-FEDER-007633 (ISISE) and by funding from ACUSTUNA project ref. CTM2015-70446-R (MINECO/ERDF, EU). L. Godinho acknowledges the financial support of Regional Operational Programme CENTRO2020 within the scope of the project CENTRO-01-0145-FEDER-000006 (SUSpENsE). I. Pérez-Arjona acknowledges the financial support of Generalitat Valenciana by grant BEST/2018/119.

REFERENCES

[1] MacLennan, David, and E. John Simmonds. Fisheries acoustics. Vol. 5. Springer Science & Business Media, 2013.

[2] MacLennan, David N. "Acoustical measurement of fish abundance". The Journal of the Acoustical Society of America 87.1 (1990): 1-15.

[3] Exactus technical Report: "EXACTUS RA 1 T1.1 Technology survey" (https://www.sintef.no/globalassets/upload/fiskeri_og_havbruk/havbruksteknologi/exactus/document/exactus_ra1_t11.pdf), accessed 2016/05/09.

[4] Pérez-Arjona, I., Godinho, L., & Espinosa, V. (2018). Numerical Simulation of Target Strength Measurements from Near to Far Field of Fish Using the Method of Fundamental Solutions. Acta Acustica united with Acustica, 104(1), 25-38.

[5] Macaulay, Gavin J., et al. "Accuracy of the Kirchhoff-Approximation and Kirchhoff-Ray-Mode Fish Swimbladder Acoustic Scattering Models." PloS one 8.5 (2013): e64055.

[6] Chen, W., & Wang, F. Z. (2010). A method of fundamental solutions without fictitious boundary. Engineering Analysis with Boundary Elements, 34(5), 530-532.

[7] Fu, Z. J., Chen, W., Chen, J. T., & Qu, W. Z. (2014). Singular boundary method: three regularization approaches and exterior wave applications. Computer Modeling in Engineering & Sciences, 0, 0, 1-26.

[8] Qu, W., Chen, W., & Gu, Y. (2015). Fast multipole accelerated singular boundary method for the 3D Helmholtz equation in low frequency regime. Computers & Mathematics with Applications, 70(4), 679-690.

[9] Anderson, V.C., (1950). Sound scattering from a fluid sphere. The Journal of the Acoustical Society of America, 22(4), 426-431.